Landslides caught on Seismic Networks and Satellite Radars

Andrea Manconi[1,2]*, Alessandro C. Mondini[3], and the ALPARRAY Working Group

[1]Department of Earth Sciences, Engineering Geology, ETH Zurich, Switzerland

[2]GAMMA Remote Sensing AG, Guemligen, Switzerland

[3]National Research Council, Istituto di Ricerca per la Protezione Idrogeologica, Perugia, Italy

*andrea.manconi@erdw.ethz.ch

ABSTRACT

Information on when, where and how landslides events occur is the key to build complete catalogues and perform accurate hazard assessments. Despite recent efforts, quantitative datasets are rare. Here we present a procedure to detect landslide events by jointly analyzing data acquired from regional broadband seismic networks and spaceborne radar imagery. To validate the method, we consider a series of six slope failures associated to the Piz Cengalo rock avalanche recently occurred in the Swiss Alps, a region where we can benefit from high spatial density and quality of seismic data, as well as from the high spatial and temporal resolution of the ESA Copernicus Sentinel-1 radar satellites. The operational implementation of the proposed approach, in combination with the future increase in availability of seismic and satellite data, can offer a new and efficient solution to build and/or expand landslide catalogues based on quantitative measurements, which are the base of hazard assessment and early warning systems at regional scale.

INTRODUCTION

Landslides cause globally fatalities and devastation, with remarkable effects on low-income and/or developing countries [1]. While the spatial occurrence of landslides is related to intrinsic geo-morphological, and climatic characteristics [2], catastrophic failures arise when slope materials reach a critical damage state [3]. In many cases, the ultimate trigger towards failure events is related to anthropic activities, extreme meteorological events, and earthquakes [4–6].

Quantitative and accurate data on timing, location and size of landslides events are crucial to study the relationships between local and regional preconditioning factors, to recognize potential causes, as well as to identify the potential effects of climatic forcing. Moreover, efficient early warning systems at regional scale rely on the availability of accurate and complete landslide catalogues [7]. Despite recent efforts, the knowledge on spatial and temporal landslide distribution is often incomplete. The information about landslide volume, runout, velocity, etc. is usually available only when the events threat life or damage infrastructures, as well as when they are associated with large earthquakes or exceptional meteorological occurrences. These catalogues, however, deliver only a partial picture of the impact of such events on the landscape. In addition, many landslide events are unreported because they occur in remote regions and do not have immediate and/or relevant impacts on human activities. This strongly hinders the completeness of inventories used for hazard assessment and for calibration of early warning systems at regional scales [8].

In recent years, two methods are emerging in the panorama of landslide event detection, i.e. satellite remote sensing and seismic data analyses. This is mainly due to the increased availability and quality of these datasets at global scale, as well as to the open data access policies. In particular, Earth Observation (EO) data acquired through different satellite missions are more and more exploited by systematic visual interpretation, as well as supervised and unsupervised automatic classification methodologies, in order to build catalogues of landslide events triggered by large

earthquakes and/or extreme meteorological events [9,10]. Further, despite the identification of signatures of landslide events in seismic networks deployed for earthquake monitoring is not a new observation [11,12], advances and diffusion of broadband seismic sensors have increased the possibility to detect and locate also landslide events of small-moderate size at regional scales. Automatic or semi-automatic procedures adapted from earthquake location routines have demonstrated good performances [13–16]; however, while uncertainties of several km can be tolerated in case of earthquake epicentral locations, landslides are extremely confined phenomena affecting a single slope (or only small portions of it). For this reason, a more accurate location of the events is necessary.

In this work, we jointly use broadband seismic data and spaceborne radar imagery to show a procedure allowing for a systematic detection and location of landslides, as well as an initial definition of their area of impact, and their magnitude. We present results over the region recently affected by the Piz Cengalo, a steep granitic massive located in the central Alps at the border between Switzerland and Italy (see Figure 1), The area was repeatedly affected by large (> 1 Mm^3), rock slope failure processes in the past decades, with the main event on August 23, 2017, being the largest (>3 Mm^3) and most catastrophic reported in recent years, causing 8 fatalities as well as damages in the range of 50M$. The Piz Cengalo slope failure is an exemplary case study to demonstrate the potential of the combination of seismic and spaceborne radar data to provide quantitative information on landslide occurrence in an alpine scenario, where we benefit from the high spatial density of the AlpArray seismic network[17] and from the unprecedented spatial and temporal resolution of Sentinel-1 Synthetic Aperture Radar (SAR) imagery[18]. A detailed description of the slope failure, its preconditioning factors, potential causes, dynamics, and the subsequent generation of a debris flow reaching the village of Bondo is beyond the scope of this work. Thus, the readers are referred to the recent literature for more information on these specific topics [19,20].

RESULTS

Hereafter, we use the term “landquake” to define “landslide events recorded by seismic sensors”, as increasingly proposed in literature [21]. We consider a total of six landquakes occurred at Piz Cengalo between August 21 and October 10, 2017 (see Table 1). The events are characterized by different magnitude in terms of volumes and runout, and occurred all in the same slope but at different stages of the progressive failure process: LQ1 occurred two days before the main failure, three events on August 23, 2017, (LQ2-LQ4), while LQ5 about a month later and LQ6 about two months later). Figure 2 shows the distribution of the AlpArray stations and examples of the signals for the LQ2 detected at different distances from the source. The apparent velocities are on the order of 3 km/s, thus compatible with surface waves generated by surficial mass movements[14].

Figure 3 shows the results obtained by analyzing the seismic data available for the LQ2 event. This is the largest landquake, and its seismic signature was detected by tens of stations up to ~500 km

distance from the source. From the seismic signal detected at multiple stations, we compute a "Likelihood of Landquake Location" function (LLL, see details in the Methods section), which results approximately centered on Piz Cengalo massive. The area within LLL>0.95 is in the order of 10,000 km^2, i.e. ~1% of the entire seismic network considered (the AlpArray covers ~1 Million km^2). However, this is still very large for an accurate identification of the LQ2 slope failure event, which affected a total area of about 1 km^2.

The initial candidate region defined by the LLL function is used to identify the available Sentinel-1 SAR imagery in terms of time of acquisition and orbit. In this specific case, the suitable orbits are the T015, ascending, and T066, descending, respectively. Then, a change detection segmentation processing is carried out (see details in the Methods section) only in the area with LLL>0.95, which is about 20% of the acquired SAR scene. Figure 4 shows our best results of the change detection analysis obtained on the ascending T015 imagery (see Supplementary Information, Table S2). Due to the temporal proximity of the LQ1-LQ4 sequence (occurred within two days, see Table 1), the LQ2 event could not be singularly discriminated, because the Sentinel-1 constellation revisit time is of six days. The LQ2, however, has been certainly the main cause of the detected surface changes. The outlier segment that identified covers an area of ~0.9 km^2, about two orders of magnitude larger than the average areas of the segment's distribution. The footprint and the dimensions of this segment are in very good agreement with the area affected by the rock avalanche[20]. The events LQ5 and LQ6 are smaller in magnitude, and the changes on the SAR image cannot be univocally defined as for the LQ2 (see Supplementary Information, Figure S2 and Figure S3). Nevertheless, the location of the largest segments identified within the Bondasca valley fall very near to the area affected by the Piz Cengalo landquake sequence.

DISCUSSION

Seismic data are capable to provide an indirect evidence of the time of landquake occurrence also in inaccessible locations, but independent validation is necessary for event confirmation and classification [22]. On the other hand, remote sensing data can deliver direct evidence of the areas hit by slope failure events, but independent observations are necessary to identify the exact time of occurrence [23]. We propose an approach exploiting seismic and remote sensing (specifically, space borne SAR data), which is suitable for the development of automatic pipelines aimed at a systematic identification, location and first evaluation of landquakes. We have shown as an exemplary case the application to a sequence of events recently occurred in the Swiss Alps. In the following we discuss the benefits and potential limitations of our approach, also in case of use in operational scenarios.

We have applied a STA/LTA approach for the identification of the event on a arbitrarly constrained temporal window (see details in the Methods section). This method has shown to be suitable for the automatic detection of mass movements in continuous seismic records also for early warning purposes, although specific calibration of the parameters used is necessary and depend on the

sensors, the network configuration, and local conditions [24]. One of the main arguments against the use of the STA/LTA approach in the detection of mass movent signals lies in the inaccuracy for the determination of the seismic event's onset, which might cause errors on the subsequent location procedures [16]. In our pipeline, however, the basic proximity approach is enough to constrains reasonably well the candidate location for all six LQ to trigger the change detection task. Furthermore, inaccuracies up to one second on the detection of the signal onset that would cause large inaccuracies in location routines based on seismic data only, would cause only negligible changes on the LLL function. (see also Supplementary Information, Figure S1). This result is possible only when a high spatial density of seismic sensors is available, such as in the AlpArray network. More advanced location routines can be applied, but homogenization of procedures across large areas like entire alpine chain is not straightforward. In addition, an increased level of complexity would not correspond to an obvious increase of accuracies for landslide location.

Another important concern after event detection is the distinction and/or classification of the signals recorded in continuous seismic waveforms (e.g., earthquakes, explosion, mass movements, anthropic sources, etc.). Several authors proposed empirical based relationships, signal processing and/or or machine learning strategies, achieving good performances [25–27]. Here we considered the method proposed in [28] based on the ratio between the local magnitude and the duration magnitude, to distinguish between local earthquakes and landquakes. The results show that with this approach the Piz Cengalo sequence could have been all automatically classified as landquakes (see Table 1). This strategy, including the evaluation of landquake volumes based on its empirical relationship observed with the duration magnitude, has been recently implemented in an operational regional system in Taiwan showing positive results [29].

As far as the change detection analysis on the Sentinel-1 SAR data is concerned, the location and mapping of landquakes as the LQ2 (i.e. in this case the LQ1-LQ4 sequence) is straightforward. The event is large and causes a relevant drop of the backscattering coefficient in the post event image, spatially over sizing the surrounding random changes always present in SAR images (speckling-like effect). Furthermore, other environmental changes in the area were not large, and in this specific case, mostly showing an increase of the backscattering coefficient. The results of the segmentation are unambiguous in all the images whatever the acquisition mode and the polarization are, even if the final segments can be slightly different. Additionally, post processing, like smoothing or gap-filling filtering, can also change partially the final shape of the segment and the identified area. On the contrary, the identification and mapping of the LQ5 and LQ6 events shows more complexity and it is not nonambiguous. According to seismic data, their sizes are smaller compared to LQ2, and then corresponding changes of the backscattering coefficient are expected to be thus less prominent in the bulk of random speckles. When the signs left on the SAR image amplitude have a size comparable the speckling-like segments, landslides cannot be univocally recognized. Regarding LQ5, the entire area of investigation is also affected by distributed environmental changes dropping the backscattering coefficient, which can be caused by snow and/or other atmospheric disturbances. Only a supervised post processing (further filtering) over the valley, which facilitated the segmentation, allowed to highlight a potential

cluster of interest. For LQ6, a small but clear signal is present in the catchment, along the slope, but is not the largest in size considering the entire distribution of segments. We note that there are other signals present in the neighboring valleys that could mislead a fully automatic analysis. For LQ5 and LQ6, the signals emerge only in the ascending imagery with VH polarization, i.e. another possible indication of the change of roughness along the slope[30]. A potential adaption for the operational implementation of our approach could be running the change detection task on progressively increasing LLL thresholds (e.g., 0.95, 0.975, etc.) and build different possible scenarios. This could provide additional hints on hot-spots, which can be verified with subsequent SAR acquisitions and/or supplementary remote sensing imagery (e.g., space-borne or air-borne). The key message of this study is to show how the systematic combination of seismic and remote sensig data can be useful for identification and mapping of landslide events. The use of Sentinel-1 SAR satellites shows the advantages of all weather, day and night, and systematic acquisitions at global scale. When available, optical imagery and/or SAR imagery acquired with different bands, full polarimetric, or with higher spatial resolution can eventually contribute to an increase the quality and the quantity of the information.

We conclude remarking that our approach is not intended to be used for early recognition of landslides or as early warning tool. The main goal of an operational implementation is to systematically populate landslide catalogues relying on quantitative and accurate information on timing, magnitude, and frequency also in remote areas. Improved catalogue completeness is very important for the calibration of regional early warning systems based on rainfall thresholds, as well as on regional hazard assessments[8]. The availability of remote sensing imagery with daily or sub-daily revisit times could lead to an employment in early detection of landslide events and possibly also in disaster response scenarios, but these potential applications have to be evaluated in future studies.

METHODS

Seismic data processing

The Swiss Seismological Service (SED) routinely recognizes landslide phenomena in seismic records of stations located in Switzerland and in the vicinity of the national borders. Despite monitoring procedures are not optimized to detect mass movements, these are systematically reported. After an event detection (at least 3 stations triggered on the SED network), a first order manual solution is obtained by identifying coherent energy at multiple stations, identifying these typically as S-waves, by using a regional 3D velocity model. In general, locations are more accurate when seismic stations are close to the event and there is good azimuthal distribution of

observations. For the Piz Cengalo landquake event associated to the largest failure (LQ2), the closest station is at ~25km and the location accuracy has uncertainties on the order of ±5 km.

To perform our back analysis on the Piz Cengalo sequence, we define a temporal window of 10 minutes centered on the date and time provided by SED with the manual procedure described above. We consider the waveforms recorded by all the AlpArray broadband stations available for each event and focused on the HHZ channel (i.e., the vertical velocity component of high broad band sampled at or above 80Hz, generally 100 or 200 Hz). The choice of the HHZ channel is justified by previous studies showing that such component usually entails the largest energy in case of landquakes[14]. We apply a STA/LTA detection (see details and parameters in the Supplementary Information, Table S1) to find the onset time of the event at each station. Then, we compute the time delay between the first triggered station, assumed to be the closest to the event, and all the other stations identifying an event in the same temporal window. The resulting values are interpolated on a regular grid of 0.25 x 0.25 degrees, spatially smoothed with an average filter (3x3 kernel), and then normalized to obtain a new function defined here as "Likelihood of Landquake Location" (LLL). The candidate region of interest (ROI) potentially affected by a landquake is defined by considering LLL>0.95, and to target the change detection processing on a spatial subset of available Sentinel-1 radar scenes.

Sentinel-1 SAR data processing

Here we adopt the change detection processing proposed in [31], here specifically modified to tackle single events instead of populations of landslides. The analysis is performed to identify potential variations of surface backscattering occurred between the pre- and post-event images, over the area with LLL>0.95 (projected into SAR coordinates). After data acquisition, pre-processing of the radar imagery includes radiometric, and geometric corrections, multi-looking, and filtering of the intensity values to obtain the radar brightness coefficient (Beta Nought, β_0) with a cell resolution of about 14 m x 14 m. Changes of β_0 have demonstrated to be a suitable indicator for the detection of landslide events of different size and occurred in different geographic scenarios (Mondini et al., 2019). In the maps of β_0, changes, landslides appear as clusters of similar values in a bulk of speckles. The β_0 changes map is then segmented using a parametric watershed approach [32] in which the scale level and the moving window kernel size parameters of the intensity algorithm are automatically assigned minimizing a cost function. The segmentation process is aimed at identifing in the candidate area LLL>0.95 a unique segment (i.e., the largest, potentially delineating changes associated to the landquake) and a number of small segments intercepting the speckle-like effect present in the β_0 changes map. Thus, the landquake is recognized as an outlier in the segment's distribution of the areas. The boundaries of the outlier segment, re-projected from SAR to ground coordinates, provide the potential location of the landquake.

References

1. Froude, M. J. & Petley, D. N. Global fatal landslide occurrence from 2004 to 2016. *Nat. Hazards Earth Syst. Sci.* **18**, 2161–2181 (2018).
2. Stead, D. & Wolter, A. A critical review of rock slope failure mechanisms: The importance of structural geology. *J. Struct. Geol.* **74**, 1–23 (2015).
3. Petley, D. N. The evolution of slope failures: mechanisms of rupture propagation. *Nat Hazards Earth Syst Sci* **4**, 147–152 (2004).
4. Bayer, B., Simoni, A., Mulas, M., Corsini, A. & Schmidt, D. Deformation responses of slow moving landslides to seasonal rainfall in the Northern Apennines, measured by InSAR. *Geomorphology* **308**, 293–306 (2018).
5. Huang Mong-Han *et al.* Coseismic deformation and triggered landslides of the 2016 Mw 6.2 Amatrice earthquake in Italy. *Geophys. Res. Lett.* **44**, 1266–1274 (2017).
6. Lacroix, P., Dehecq, A. & Taipe, E. Irrigation-triggered landslides in a Peruvian desert caused by modern intensive farming. *Nat. Geosci.* 1–5 (2019) doi:10.1038/s41561-019-0500-x.
7. Gariano, S. L. & Guzzetti, F. Landslides in a changing climate. *Earth-Sci. Rev.* **162**, 227–252 (2016).
8. Guzzetti, F. *et al.* Geographical landslide early warning systems. *Earth-Sci. Rev.* 102973 (2019) doi:10.1016/j.earscirev.2019.102973.
9. Mondini, A. C. *et al.* Sentinel-1 SAR Amplitude Imagery for Rapid Landslide Detection. *Remote Sens.* **11**, 760 (2019).
10. Tanyaş, H. *et al.* Presentation and Analysis of a Worldwide Database of Earthquake-Induced Landslide Inventories. *J. Geophys. Res. Earth Surf.* **122**, 2017JF004236 (2017).
11. Govi, M., Gullà, G. & Nicoletti, P. G. Val Pola rock avalanche of July 28, 1987, in Valtellina (Central Italian Alps). in *Reviews in Engineering Geology* vol. 15 71–90 (Geological Society of America, 2002).
12. Weichert, D., Horner, R. B. & Evans, S. G. Seismic signatures of landslides: The 1990 Brenda Mine collapse and the 1965 hope rockslides. *Bull. Seismol. Soc. Am.* **84**, 1523–1532 (1994).
13. Chao, W.-A. *et al.* A first near real-time seismology-based landquake monitoring system. *Sci. Rep.* **7**, (2017).
14. Dammeier, F., Moore, J. R., Haslinger, F. & Loew, S. Characterization of alpine rockslides using statistical analysis of seismic signals. *J. Geophys. Res. Earth Surf.* **116**, F04024 (2011).
15. Ekstrom, G. Global Detection and Location of Seismic Sources by Using Surface Waves. *Bull. Seismol. Soc. Am.* **96**, 1201–1212 (2006).
16. Fuchs, F., Lenhardt, W., Bokelmann, G. & the AlpArray Working Group. Seismic detection of rockslides at regional scale: examples from the Eastern Alps and feasibility of kurtosis-based event location. *Earth Surf. Dyn.* **6**, 955–970 (2018).
17. Hetényi, G. *et al.* The AlpArray Seismic Network: A Large-Scale European Experiment to Image the Alpine Orogen. *Surv. Geophys.* **39**, 1009–1033 (2018).
18. Torres, R. *et al.* GMES Sentinel-1 mission. *Remote Sens. Environ.* **120**, 9–24 (2012).
19. Mergili, M., Jaboyedoff, M., Pullarello, J. & Pudasaini, S. P. Back-calculation of the 2017 Piz Cengalo-Bondo landslide cascade with r.avaflow. *Nat. Hazards Earth Syst. Sci. Discuss.* 1–30 (2019) doi:https://doi.org/10.5194/nhess-2019-204.

20. Walter, F. *et al.* Direct observations of a three million cubic meter rock-slope collapse with almost immediate initiation of ensuing debris flows. *Geomorphology* 106933 (2019) doi:10.1016/j.geomorph.2019.106933.
21. Chen, C.-H. *et al.* A seismological study of landquakes using a real-time broad-band seismic network. *Geophys. J. Int.* **194**, 885–898 (2013).
22. Ekström, G. & Stark, C. P. Simple scaling of catastrophic landslide dynamics. *Science* **339**, 1416–1419 (2013).
23. Guzzetti, F. *et al.* Landslide inventory maps: New tools for an old problem. *Earth-Sci. Rev.* **112**, 42–66 (2012).
24. Coviello, V., Arattano, M., Comiti, F., Macconi, P. & Marchi, L. Seismic Characterization of Debris Flows: Insights into Energy Radiation and Implications for Warning. *J. Geophys. Res. Earth Surf.* **124**, 1440–1463 (2019).
25. Dammeier, F., Moore, J. R., Hammer, C., Haslinger, F. & Loew, S. Automatic detection of alpine rockslides in continuous seismic data using Hidden Markov Models. *J. Geophys. Res. Earth Surf.* 2015JF003647 (2016) doi:10.1002/2015JF003647.
26. Hibert, C., Michéa, D., Provost, F., Malet, J.-P. & Geertsema, M. Exploration of continuous seismic recordings with a machine learning approach to document 20 yr of landslide activity in Alaska. *Geophys. J. Int.* **219**, 1138–1147 (2019).
27. Moore, J. R. *et al.* Dynamics of the Bingham Canyon rock avalanches (Utah, USA) resolved from topographic, seismic, and infrasound data. *J. Geophys. Res. Earth Surf.* 2016JF004036 (2017) doi:10.1002/2016JF004036.
28. Manconi, A., Picozzi, M., Coviello, V., De Santis, F. & Elia, L. Real-time detection, location, and characterization of rockslides using broadband regional seismic networks. *Geophys. Res. Lett.* **43**, 2016GL069572 (2016).
29. Chang, J.-M., Chao, W.-A., Chen, H., Kuo, Y.-T. & Yang, C.-M. Locating rock slope failures along highways and understanding their physical processes using seismic signals. *Earth Surf. Dyn. Discuss.* 1–20 (2020) doi:https://doi.org/10.5194/esurf-2020-94.
30. Sung, C. C. & Holzer, J. A. Scattering of electromagnetic waves from a rough surface. *Appl. Phys. Lett.* **28**, 429–431 (1976).
31. Mondini, A. C. Measures of Spatial Autocorrelation Changes in Multitemporal SAR Images for Event Landslides Detection. *Remote Sens.* **9**, 554 (2017).
32. Roerdink, J. B. T. M. & Meijster, A. The Watershed Transform: Definitions, Algorithms and Parallelization Strategies. *Fundam. Informaticae* **41**, 187–228 (2000).

Author Contributions

AM and ACM equally contributed to the conceptualization of the investigation. AM analyzed and interpreted the seismic data. ACM analyzed and interpreted the Sentinel-1 imagery. AM and ACM wrote and revised the manuscript.

Consortium

The AlpArray Working group is responsible for the seismic stations installation, mantainance, and for seismic data curation. The components of the AlpArray Working group are listed below (updated 23 January 2021):

György HETÉNYI, Rafael ABREU, Ivo ALLEGRETTI, Maria-Theresia APOLONER, Coralie AUBERT, Simon BESANÇON, Maxime BÈS DE BERC, Götz BOKELMANN, Didier BRUNEL, Marco CAPELLO, Martina ČARMAN, Adriano CAVALIERE, Jérôme CHÈZE, Claudio CHIARABBA, John CLINTON, Glenn COUGOULAT, Wayne C. CRAWFORD, Luigia CRISTIANO, Tibor CZIFRA, Ezio D'ALEMA, Stefania DANESI, Romuald DANIEL, Anke DANNOWSKI, Iva DASOVIĆ, Anne DESCHAMPS, Jean-Xavier DESSA, Cécile DOUBRE, Sven EGDORF, ETHZ-SED Electronics Lab, Tomislav FIKET, Kasper FISCHER, Wolfgang FRIEDERICH, Florian FUCHS, Sigward FUNKE, Domenico GIARDINI, Aladino GOVONI, Zoltán GRÁCZER, Gidera GRÖSCHL, Stefan HEIMERS, Ben HEIT, Davorka HERAK, Marijan HERAK, Johann HUBER, Dejan JARIĆ, Petr JEDLIČKA, Yan JIA, Hélène JUND, Edi KISSLING, Stefan KLINGEN, Bernhard KLOTZ, Petr KOLÍNSKÝ, Heidrun KOPP, Michael KORN, Josef KOTEK, Lothar KÜHNE, Krešo KUK, Dietrich LANGE, Jürgen LOOS, Sara LOVATI, Deny MALENGROS, Lucia MARGHERITI, Christophe MARON, Xavier MARTIN, Marco MASSA, Francesco MAZZARINI, Thomas MEIER, Laurent MÉTRAL, Irene MOLINARI, Milena MORETTI, Anna NARDI, Jurij PAHOR, Anne PAUL, Catherine PÉQUEGNAT, Daniel PETERSEN, Damiano PESARESI, Davide PICCININI, Claudia PIROMALLO, Thomas PLENEFISCH, Jaroslava PLOMEROVÁ, Silvia PONDRELLI, Snježan PREVOLNIK, Roman RACINE, Marc RÉGNIER, Miriam REISS, Joachim RITTER, Georg RÜMPKER, Simone SALIMBENI, Marco SANTULIN, Werner SCHERER, Sven SCHIPPKUS, Detlef SCHULTE-KORTNACK, Vesna ŠIPKA, Stefano SOLARINO, Daniele SPALLAROSSA, Kathrin SPIEKER, Josip STIPČEVIĆ, Angelo STROLLO, Bálint SÜLE, Gyöngyvér SZANYI, Eszter SZŰCS, Christine THOMAS, Martin THORWART, Frederik TILMANN, Stefan UEDING, Massimiliano VALLOCCHIA, Luděk VECSEY, René VOIGT, Joachim WASSERMANN, Zoltán WÉBER, Christian WEIDLE, Viktor WESZTERGOM, Gauthier WEYLAND, Stefan WIEMER, Felix WOLF, David WOLYNIEC, Thomas ZIEKE, Mladen ŽIVČIĆ, Helena ŽLEBČÍKOVÁ

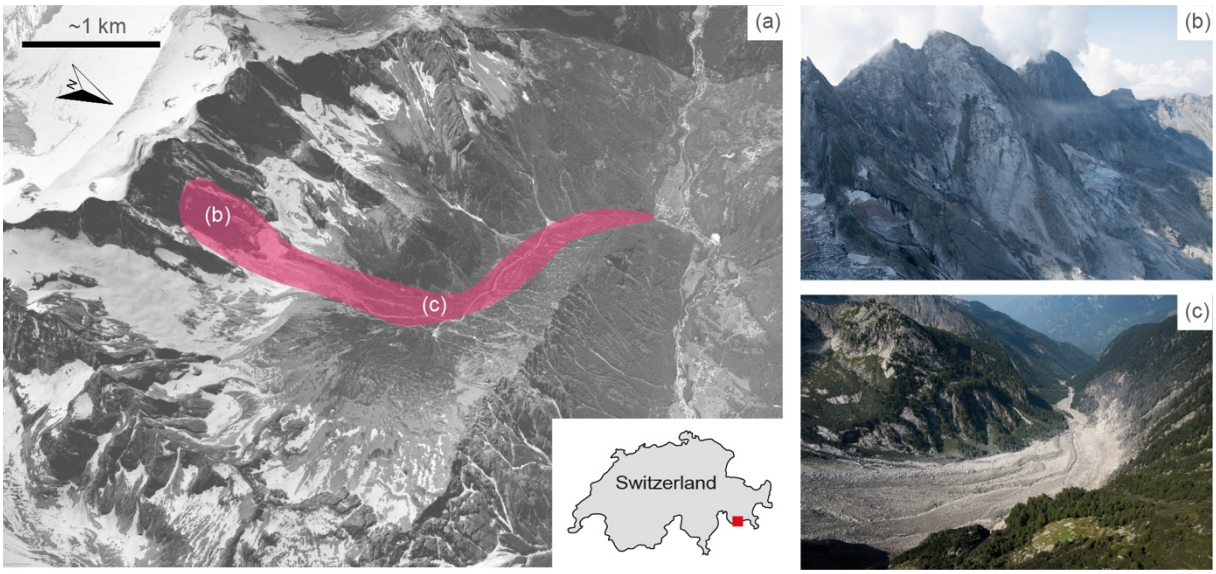

Figure 1. Overview of the area of investigation. (a) Google Earth© view of the Val Bondasca, with approximate outline of the area affected by the Piz Cengalo (46.29475° N, 9.602056° E) rock avalanche and subsequent debris flows; (b) Detail of the release area, August 25, 2017; (c) Detail of the deposits, August 30 2017. © Photos VBS swisstopo Flugdienst.

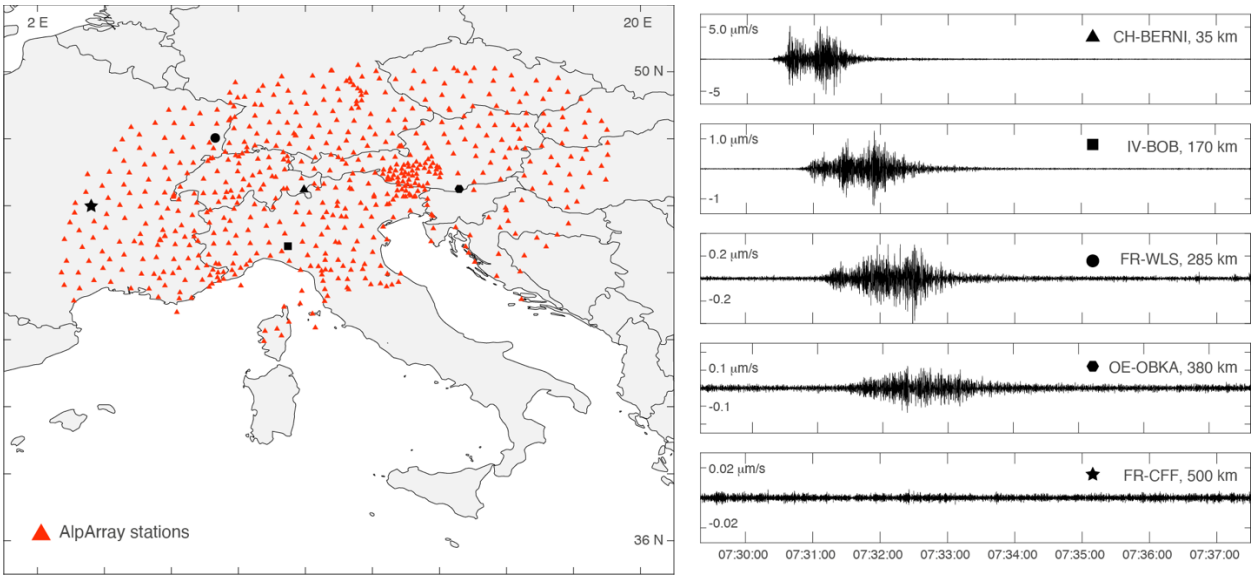

Figure 2. Seismic network and data (left) The AlpArray network of broad band stations. (right) Selected signals (vertical component HHZ) recorded by AlpArray stations located at different distances from event LQ2 (see Table 1), occurred on August 23, 2017 (i.e., the main Piz Cengalo rock avalanche event).

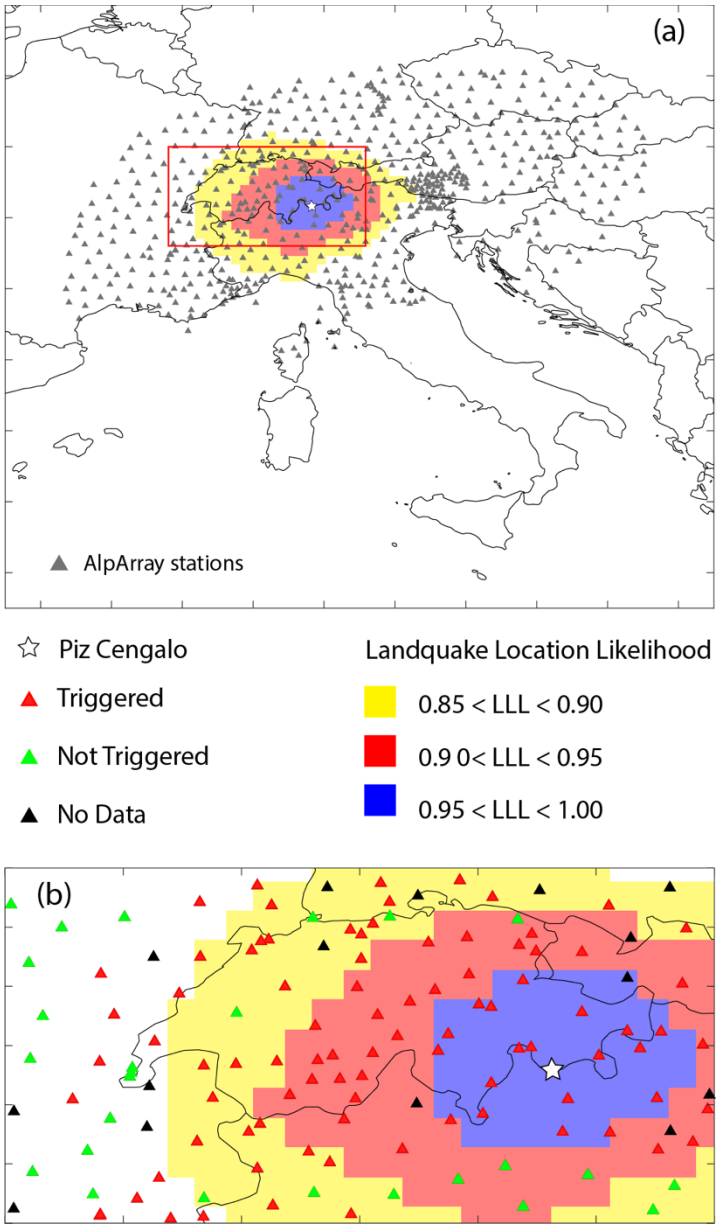

Figure 3. Likelihood of Landquake Location (LLL) based on the arrival time of seismic signals recorded by AlpArray stations. This basic analysis of the seismic data is used to constrain the approximate location where a landslide event has occurred. (a) LLL over the entire AlpArray network (b) Zoom on the areas with high likelihood. The area 0.95<LLL<1.0 is used to confine the change detection analysis. True location of the Piz Cengalo event (white star) is also shown.

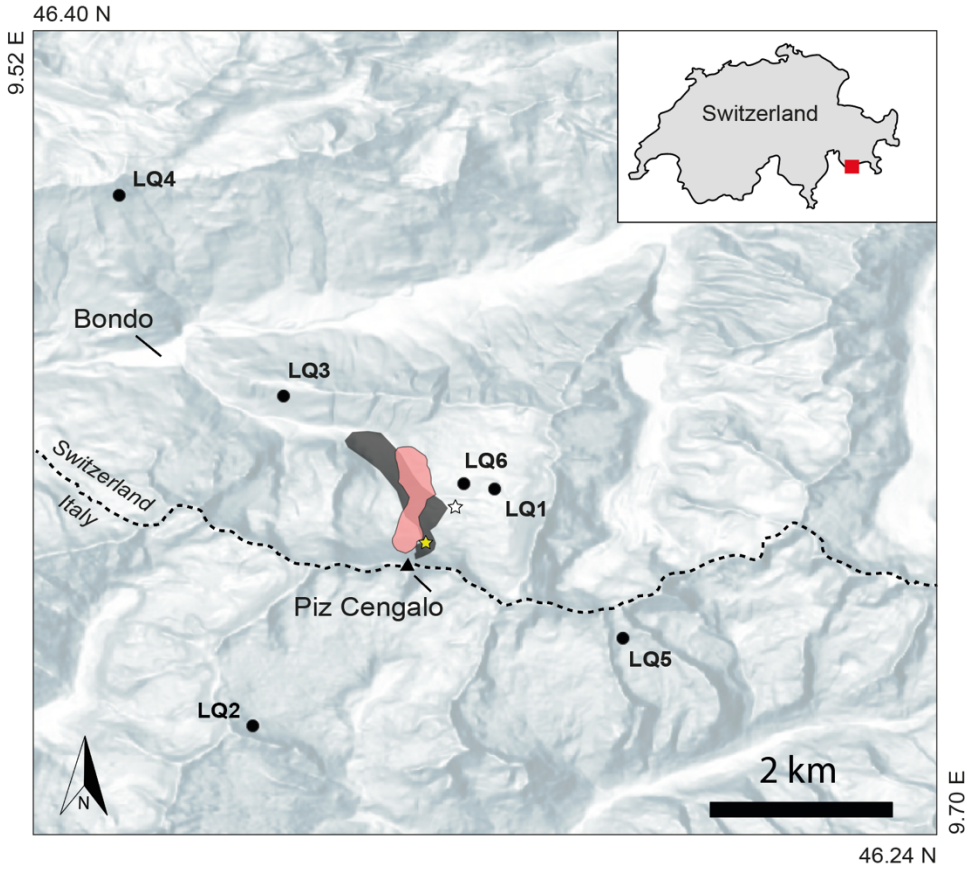

Figure 4. Results of the change detection analysis. The red polygon shows the area identified as potential landquake location for the main Landquake event (i.e., LQ1-LQ4) identified by processing the Sentinel-1 pre- and post-event, while the gray polygon is the area hit by the rock avalanche. The white star and the yellow star show the locations of the largest segments for LQ5 and LQ6, respectively, identified within the Bondasca valley.The black dots show the epicentral locations provided by SED (see Table 1).

Event ID	Date/Time (UTC)	ML	MD*	ML/MD	Vol (Mm3)
LQ1	2017-08-21T09:29:09	2.3	3.03	0.75	0.078 - 0.167
LQ2	2017-08-23T07:30:27	3.0	3.71	0.80	1.65 - 2.61
LQ3	2017-08-23T09:03:57	1.3	2.86	0.45	0.02 - 0.14
LQ4	2017-08-23T09:36:16	2.1	3.22	0.65	0.12 - 0.50
LQ5	2017-09-15T20:04:36	2.3	3.26	0.70	0.23 - 0.41
LQ6	2017-10-10T02:58:41	1.1	2.65	0.41	0.014 - 0.035

Table 1. Summary of the landquakes analyzed in this study and associated to the Piz Cengalo slope failure. ML are estimated by SED, while average magnitude duration (MD) and volumes are computed following[28], by considering the event duration on all triggered AlpArray stations. Note that all LQ events have ML/MD have ML/MD less or equal to 0.8, i.e. they can be discerned from earthquake events which typically have ML/MD ~ 1.